HHS Public Access

Author manuscript

ACS Biomater Sci Eng. Author manuscript; available in PMC 2020 October 14.

Published in final edited form as:

ACS Biomater Sci Eng. 2019 October 14; 5(10): 5327–5336. doi:10.1021/acsbiomaterials.9b00810.

Hyperosmolar potassium inhibits myofibroblast conversion and reduces scar tissue formation

Jonathan M. Grasman[1], **Marisa D. Williams**[1], **Constantine G. Razis**[1], **Mattia Bonzanni**[1,4], **Anne S. Golding**[2], **Dana M. Cairns**[1], **Michael Levin**[3,4], **David L. Kaplan**[1,4,*]

[1]Department of Biomedical Engineering, Tufts University, Medford, Massachusetts 02155

[2]Department of Chemical and Biological Engineering, Tufts University, Medford, Massachusetts 02155

[3]Department of Biology, Tufts University, Medford, Massachusetts 02155

[4]Allen Discovery Center, Tufts University, Medford, Massachusetts 02155

Abstract

Scar formation is a natural result of almost all wound healing in adult mammals. Unfortunately, scarring disrupts normal tissue function and can cause significant physical and psychological distress. In addition to improving surgical techniques to limit scar formation, several therapies are under development towards the same goal. Many of these treatments aim to disrupt transforming growth factor β1 (TGFβ1) signaling, as this is a critical control point for fibroblast differentiation into myofibroblasts; a contractile cell that organizes synthesized collagen fibrils into scar tissue. The present study aimed to examine the role of hyperosmolar potassium gluconate (KGluc) on fibroblast function in skin repair. KGluc was first determined to negatively regulate fibroblast proliferation, metabolism, and migration in a dose-dependent manner *in vitro*. Increasing concentrations of KGluc also inhibited differentiation into myofibroblasts, suggesting that local KGluc treatment might reduce fibrosis. KGluc delivery was confirmed via loading into collagen hydrogels and used to treat a full thickness skin wound in mice. KGluc qualitatively slowed initial closure of the wounds and resulted in tissue that more closely resembled mature, healthy skin (epidermal thickness and dermal-epidermal morphology) when compared to unloaded collagen hydrogels. KGluc treatment significantly reduced the number of myofibroblasts within the dermis while upregulated blood vessel density with respect to unloaded hydrogels, likely a result of disruption of TGFβ1 signaling. Taken together, these data demonstrate the effectiveness of KGluc treatment on skin wound healing and suggest that this may be an efficient treatment to limit scar formation.

*Address Correspondence to: David L. Kaplan, Ph.D., Department of Biomedical Engineering, Tufts University, 4 Colby St, Medford, MA, 02155, Tel: 617-627-3251, Fax: 617-627-3231, david.kaplan@tufts.edu.

AUTHOR CONTRIBUTIONS

J.M.G. conceived the idea, performed experiments and data analysis, and wrote the paper. M.D.W., C.G.R., M.B., A.S.G., and D.M.C. performed experiments and data analysis. D.L.K. and M.L. supervised the project. All authors edited the manuscript.

SUPPORTING INFORMATION

Titration of TGFβ1 on fibroblast differentiation; effect of supplementation of additional hyperosmolar salts on fibroblast differentiation

COMPETING INTERESTS

The authors declare no competing financial or non-financial interests.

Graphical Abstract

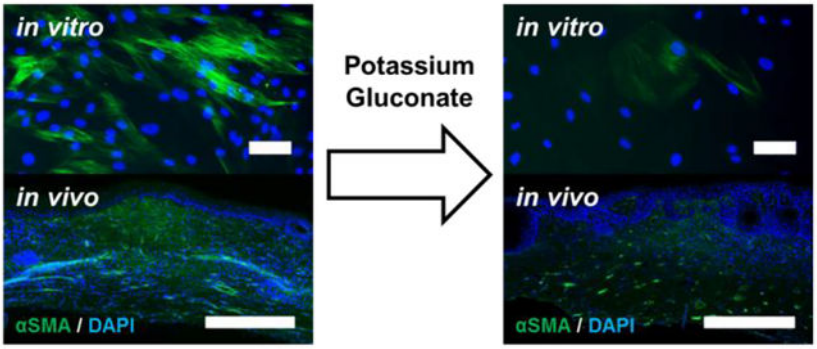

Keywords

skin regeneration; anti-fibrosis; potassium gluconate; wound healing; myofibroblasts

1. INTRODUCTION

Adult mammalian wound healing almost always results in scar formation. While this may facilitate enhanced strength in load bearing tissues,[1] it is also an incredibly important consideration for cosmetic and reconstructive procedures.[2] For instance, there are almost 200,000 reconstructive surgeries solely focused on scar removal, notwithstanding the significant effort to employ surgical techniques to reduce scar formation in the first place.[3] In these cases, the prevention of scar tissue formation is critical to ensure aesthetic preservation of facial structures. Native skin regeneration occurs with fibroblasts infiltrating the wound site to repair and replace damaged or missing extracellular matrix (ECM). Once the replaced ECM is present, keratinocytes migrate and re-epithelize the defect. While small, partial defects can be repaired by the skin's innate regeneration mechanisms, often there is dysregulation of the regeneration process with complete thickness, or critically sized defects. The main cause of dysregulation in these cases is a surplus of collagen (mainly type I) deposition, and subsequent reorganization of the collagen fibrils, by myofibroblasts.[4] Resident fibroblasts convert to a myofibroblast phenotype when exposed to factors such as transforming growth factor β1 (TGFβ1) and while a certain number of myofibroblasts are necessary for wound healing, increased numbers have been shown to result in increased scar tissue formation.[5] Therefore, there is a need to understand how to promote skin regeneration while reducing myofibroblasts conversion to limit scar formation.

Several therapies are under development to potentially limit scar formation and fibrosis in natural wound healing. These approaches range from pharmacologic interventions (e.g. tacrolimus, losartan, curcumin) to tissue engineered constructs incorporating bioactive molecules (e.g. MG53, a tripartite motif family protein involved in cell membrane repair machinery, or proteoglycans).[4, 6] These interventions usually target one of 3 mechanisms: TGFβ1 signaling, collagen synthesis, myofibroblast activation, and/or inflammation, as each of these control points are critical for scar formation.[6] Intravenous delivery of curcumin was able to reduce scar formation in rabbit ear wounds, and was found to inhibit TGFβ1/SMAD

(homologues of the Drosophila protein, mothers against decapentaplegic (Mad) and the *Caenorhabditis elegans* protein Sma) signaling in keloid fibroblasts.[7] A disadvantage to several pharmacologic interventions such as curcumin is that they are applied systemically, which may result in undesired complications in other tissues.[7–8] To ameliorate concerns regarding systemic interventions, tissue engineered constructs provide an implantable material that can both serve as a reservoir for soluble compounds as well as deliver insoluble cues to drive cell functions. For example, delivery of MG53 via a hydrogel increased its efficacy and rate of skin closure in an *in vivo* full thickness skin injury in rats with respect to unloaded hydrogel controls.[9] Therefore, it is critical to consider both the effectiveness of a potential therapeutic compound as well as its localized, active delivery to an injury site.

Recent work conducted in our lab and others, has identified potassium gluconate (KGluc) as a powerful regulator of cell function. KGluc supplementation has been proposed as a mechanism to control differentiation of human mesenchymal stem cells (hMSCs), and was demonstrated to inhibit bone and adipose differentiation.[10–11] In addition to regulating hMSCs, KGluc has been shown to downregulate osteoarthritic markers in chondrocytes.[12] The innate immune system is a critical parameter for fibrosis and arthritis, and KGluc has also been shown to impact macrophage expression and secretion of a variety of inflammatory and immune-regulatory cytokines, such as tumor necrosis factor α (TNFα).[13] Interestingly, hyperosmolar potassium has also been shown to regulate paired box (PAX) 5 expression, which is required for pre-B cell maturation in mice and could become a treatment method for the treatment of pre-B acute lymphoblastic leukemia (ALL).[14] A hypothesized mechanism of action for KGluc on these cell types is through the electrochemical gradients maintained by potassium-permeable ion channels.[15] It is thought that renal fibrosis is also heavily regulated by potassium channels, and that regulation of potassium signaling may serve as a treatment for fibrotic kidney disease.[16] While hyperosmolar potassium has been implicated in these varied tissue systems, its role in both mesenchymal fibroblast cell function and tissue remodeling remains poorly understood.

The goal of this work was to determine the effects of hyperosmolar potassium gluconate on scar tissue formation and fibroblast differentiation into myofibroblasts. To this end, we first developed a series of *in vitro* assays utilizing primary human dermal fibroblasts. We identified that hyperosmolar potassium gluconate inhibited both proliferation and fibroblast differentiation in a dose-dependent manner. We next sought to identify an efficient method to deliver exogenous potassium gluconate in a clinical context by loading it into collagen hydrogels. Lastly, we translated our *in vitro* findings into a relevant *in vivo* model of wound healing and found that exogenous potassium gluconate in dermal wound sites modestly decreased the rate of wound closure, however, it resulted in more morphologically mature skin with significantly less myofibrobasts present in the dermis. Taken together, our data reveal a novel role for potassium gluconate in promoting skin wound healing and the prevention of scar tissue formation, which is essential for aesthetic considerations for facial reconstruction, among other potential clinical outcomes.

2. EXPERIMENTAL SECTION

2.1. Cell culture

Two sources of human neonatal foreskin fibroblasts (HFFs) were cultured in this study. One was a gift from Dr. Jonathan Garlick, and were used prior to reaching passage 7, the second line was obtained commercially (ATCC SCRC-1041; ATCC, Manassas, VA) and were used prior to reaching passage 21. HFFs were cultured in complete Dulbecco's modified Eagle Medium (DMEM) growth medium (GM; Cat. No. 10569, Gibco BRL, Gaithersburg, MD) supplemented with 10% fetal bovine serum (FBS, Gibco) and 1% anti-anti (Gibco). Cells were incubated at 37°C with 5% CO_2 and maintained using standard cell culture techniques. Routine cell passage was conducted at 80–90% confluence using 0.25% trypsin-EDTA (Gibco).

Fibroblasts were seeded into well plates at a density of 5,000 cell/cm^2 and cultured in GM for three days as a growth phase. Differentiation to myofibroblasts was induced by culturing fibroblasts in differentiation medium (DM; GM supplemented with transforming growth factor β1 (TGFβ1; R&D Systems, Minneapolis, MN)) for four days. To assess the importance of temporal delivery of compounds, fibroblasts were cultured in GM supplemented with potassium gluconate (KGluc, Sigma-Aldrich), St. Louis, MO) reconstituted in de-ionized water during the growth phase ("constant" stimulation), or only during the differentiation phase ("late" stimulation). All fibroblasts in the differentiation phase were cultured in the indicated concentrations of KGluc. At the end of each time point fibroblasts were fixed with 4% paraformaldehyde (PFA; Boston BioProducts, Ashland, MA). Each treatment condition was run in duplicate or quadruplicate per independent experiment, as indicated.

2.2. Metabolic assay

To determine the effects of hyperosmolar potassium gluconate on the metabolic activity of fibroblasts, a metabolism assay was performed at the end of both the growth phase and differentiation phase of HFFs. Fibroblasts were seeded in 96 well plates and followed the same cell culture protocols. At the end of the culture period, medium was replaced with medium supplemented with the cell counting kit 8 (CCK-8) reagent (Sigma-Aldrich), and the assay was performed according to the manufacturer's instructions. Blank wells were subtracted out of the readings and then data were normalized to the metabolic activity of control fibroblasts cultured in GM for the duration of the experiment. Each experimental condition was performed in quadruplicate.

2.3. Scratch assay

To determine the effects of hyperosmolar KGluc on the migration of fibroblasts, a scratch assay was conducted. Fibroblasts were seeded and grown to confluence. At confluence, a P200 tip was drawn across the diameter of each well to generate an *in vitro* wound. After injury, wells were rinsed with PBS to remove cellular debris and replaced with GM supplemented with indicated concentrations of KGluc. Two separate regions in each well were imaged immediately after injury and the same regions were imaged every four hours for 24 hours using a Keyence BZ-X700 microscope and associated software (Keyence,

Elmwood Park, NJ). The injured area (i.e. the portion of plates not covered by cells) was measured in Image J (NIH) and migration rates were calculated based upon the distance between the moving cell fronts. Each experimental condition was performed in duplicate.

2.4. Collagen gel fabrication

To develop a clinically relevant delivery mechanism for KGluc, KGluc was supplemented into collagen gels. As a concentration of 60 mM of KGluc was determined to be efficient to modulate fibroblast function, we calculated that 100 μL of collagen gel would need to have 1,000 mM KGluc (KG-High) to ensure the same amount was delivered in our culture conditions. As higher salinity conditions could interfere with collagen gelation, gels were also loaded with 500 mM KGluc (KG-Low). Collagen gels were fabricated as previously describe, per manufacturer's instructions.[17] Briefly, type I rat tail collagen (Corning, Corning, NY) was mixed to a final concentration of 3.0 mg/mL with 10X phosphate buffered saline (PBS; ThermoFisher, Waltham, MA), sodium hydroxide (NaOH; Sigma-Aldrich), GM, and the indicated concentration of KGluc. When fibroblasts were transitioned to DM, 100 μL of the mixed collagen solution was pipetted into transwells with a 3 μm pore size (Corning) on top of fibroblasts. Each experimental condition was performed in duplicate.

2.5. Patch clamping

Patch clamp experiments in the whole cell configuration were carried out at room temperature. Fibroblasts were superfused with either an N-methyl-D-glucamine (NMDG)-based solution (in mM: 85.4 NaCl, 54.6 NMDG, 5.4 KCl, 1.8 $CaCl_2$, 1 $MgCl_2$, 10 HEPES-NaOH, 5.5 Glucose; pH: 7.4) or a KGluc-based solution (in mM: 85.4 NaCl, 60 KGluc, 1.8 $CaCl_2$, 1 $MgCl_2$, 10 HEPES-NaOH, 5.5 Glucose; pH: 7.4); the osmolarity was thus kept constant at 322 mOsm. Patch clamp pipettes had a resistance of 5–7 MΩ when filled with an intracellular-like solution containing (in mM: 130 K-Asp, 10 NaCl, 5 EGTA-KOH, 2 $MgCl_2$, 2 $CaCl_2$, 2 ATP (Na-salt), 5 creatine phosphate, 0.1 GTP, 10 Hepes-KOH; pH: 7.2). Resting membrane potential (RMP) recordings were carried out in the I/O configuration for 30 seconds. Neither series resistance compensation nor leak correction were applied: liquid junction potential correction was applied as previously reported.[18]

2.6. In vivo wound assay

All animal protocols were approved by the Institutional Animal Care and Use Committee (IACUC) at Tufts University, and were conducted as previously reported.[19] Twelve week old female BALB/cJ mice (Jackson Laboratories, Bar Harbor, ME) were anesthetized with isofluorane and the dorsal surface was shaved and prepped for surgery. An 8 mm biopsy punch was utilized to make two round, full-thickness excisional wounds on either side of the spine. In the left side wound, 50 μL collagen gels loaded with 0 (vehicle control), 500 mM (KG-Low), or 1000 mM (KG-High) KGluc were pipetted onto the wound and allowed to solidify. The right side wounds remained untreated and served as additional internal controls. Both wounds were sealed using Tegaderm, and wound closure was followed over the course of 14 days. Tegaderm was removed from all animals at day 8 because it peeled off of some animals. At the conclusion of each study, animals were euthanized via CO_2 inhalation followed by cervical dislocation and wound site tissue was excised, fixed in 4%

paraformaldehyde, and stored in 30% (*w/v*) sucrose (Sigma) for further analysis. Three animals were used per treatment.

2.7. Immunostaining

Excised tissues were bisected, embedded in OCT compound (ThermoFisher), and serial 10 μm sections were cut and mounted onto Superfrost Plus slides (VWR, West Chester, PA). Antigen retrieval was conducted on serial sections of slides in a microwave for 20 min using a citrate-based antigen retrieval solution (Vector Laboratories, Burlingame, CA). Three or more sections spaced at least 50 μm apart were analyzed per animal, and averaged prior to statistical evaluation. The samples were allowed to cool to room temperature and rinsed with PBS. From here, treated slides and fixed cells from *in vitro* experiments were rinsed with PBS/Tween-20 (PBST, 0.05% *v/v*), permeabilized with 0.1% Triton X-100 (Sigma), blocked using 5% bovine serum albumin (BSA; Sigma) in PBST (*w/v*), and immunostained with primary antibodies against α smooth muscle actin (αSMA; 1:100, ab7817, Abcam, Cambridge, MA), Ki67 (1:500, ab15580, Abcam), or cytokeratin 10 (K10; 1:100, ab9026, Abcam) with 1% BSA in PBST. After 2 rinses with PBST, samples were incubated with species-matched Alexafluor 488 and 594 secondary antibodies (1:500, A-21202 and A-11072 respectively; ThermoFisher), counterstained with DAPI (ThermoFisher), and finally rinsed with PBS. Histology and immunostained images were collected using a Keyence BZ-X700 microscope with associated software. Quantitative analyses were performed using Image J in a double-blinded fashion. To determine the percentage of proliferating fibroblasts, five images were taken of each well and the number of Ki67 positive nuclei were normalized to the total number of nuclei present in each image.

2.8. Analysis of αSMA positive myofibroblasts

To determine the effectiveness of KGluc to reduce myofibroblast formation, cells or tissue sections were immunostained against αSMA and visualized. Five images were collected per well for *in vitro* studies and tissue sections were stitched together after collecting images using a 10X objective, highlighting the wounded tissue region. These regions of interest were opened in Image J and background fluorescence was removed after observing background intensity in all images. The resulting images were converted to binary and the percent area that was positive for αSMA staining was recorded. For the analysis of tissue sections, these measurements were normalized to the amount of DAPI staining to exclude overall cell number as a confounding variable.

2.9. Estimation of epidermal thickness

To approximate the changes in epidermal thickness, the thickness of the keratinizing layer of epidermis was measured. Images were acquired from slides stained with K10 with a 10X objective and stitched together using associated Keyence software. Images were imported into Image J and the thickness of the epidermis was measured.

2.10. Statistics

Data are reported as mean ± standard error, and sample sizes are reported as the number of independent experiments. Because the data from both fibroblast lines resulted in the same

results, they are presented in aggregate throughout this study. Statistical analyses were performed using a one-way analysis of variance (ANOVA) with $p<0.05$ indicating significant differences between groups using SigmaPlot 13.0 software (Systat Software, Inc., San Jose, CA). For post hoc analyses, a Holm-Sidak pairwise multiple comparison test was performed to determine significance between experimental groups using an overall significance level of $p<0.05$. Where indicated, a Student's t-test was performed where differences between conditions were considered significant at $p<0.05$.

3. RESULTS

3.1. Potassium gluconate inhibits fibroblast proliferation and metabolic activity

We first investigated the effects of supplementing fibroblast growth medium in increasing concentrations of potassium gluconate (KGluc) on fibroblast cell proliferation *in vitro*. Characteristic images of fibroblast cultures supplemented with KGluc suggested a reduction in cell density with 80 mM KGluc after a culture period of 3 days (Figure 1 A–D). There were no changes in the localization or expression patterns of Ki67, however, there was a significant reduction in the percentage of Ki67 positive nuclei when cultured with 60 and 80 mM KGluc with respect to control cultures without KGluc (Figure 1E). The fibroblast density also significantly decreased with these elevated KGluc concentrations (Figure 1F), which also resulted in a reduction of metabolic activity normalized to the activity in controls (Figure 1G). Importantly, KGluc significantly reduced proliferation, density, and metabolism for both primary fibroblasts and ATCC 1041 fibroblasts, so these results have been pooled throughout the study. To determine the effects of prolonged exposure to KGluc on fibroblast metabolism, fibroblasts were transitioned to differentiation medium with KGluc for 4 days after cultivation in growth medium that was either cultured with hyperosmolar potassium ("constant" culture with KGluc) or without exogenous potassium ("late" culture with KGluc) (Figure 2A). There was a significant, step-wise reduction in metabolic activity with increasing amounts of KGluc with respect to untreated controls (Figure 1H). Interestingly, constant KGluc treatment also significantly reduced metabolic activity with respect to late KGluc treatment, suggesting an importance in the timing of this intervention. It is important to note that there were no differences in the metabolism of fibroblasts cultured in growth medium for the entire experiment (white bar) and fibroblasts transitioned to differentiation medium (green bar) without KGluc, showing that the change in medium formulation did not impact these changes in cell metabolism.

3.2. Constant treatment with potassium gluconate restricts fibroblast migration

To characterize the effects of KGluc treatment on fibroblast migration, we utilized the scratch assay technique. Fibroblasts were grown either in the presence of KGluc ("constant") or without ("late") to confluency and a scratch injury was generated using a P200 pipette tip. All fibroblast cultures received KGluc supplementation after induction of the assay. Cultures were imaged immediately after injury and every four hours for 24 hours and the migration rate was calculated based upon the distance between the moving cell fronts (Figure 2B). All groups except for late exposure to 40 mM KGluc demonstrated significantly lower migration rates with respect to untreated controls. There was a step-wise reduction in the migration rate of fibroblasts exposed to increasing concentrations of KGluc

in the constant treatment group, and there was also a significant reduction in migration rate of fibroblasts in the late treatment group between 60 and 80 mM KGluc with respect to 40 mM KGluc supplementation (Figure 2C). Constant exposure to 40 and 60 mM KGluc significantly reduced the migration rate of fibroblasts with respect to late exposure conditions, while there was only a qualitative reduction at 80 mM KGluc.

3.3. Potassium gluconate inhibits fibroblast differentiation to myofibroblasts

To analyze the effects of KGluc treatment on fibroblast differentiation, we determined how exposure time and concentration of KGluc inhibited TGFβ1-mediated myofibroblast conversion. To identify the concentration of TGFβ1 necessary to convert to the myofibroblast phenotype, we incubated fibroblasts in growth medium for three days and transferred the cells to differentiation medium, which included increasing amounts of TGFβ1. All evaluated concentrations of TGFβ1 yielded α smooth muscle actin (αSMA) positive myofibroblasts (Supplementary Figure S1 A–D) while no αSMA positive myofibroblasts were observed in control cultures without TGFβ1 (Supplementary Figure S1E). The relative amount of αSMA expression as detected by immunostaining plateaued at 1 ng/mL TGFβ1 (Supplementary Figure S1F), so all future differentiation experiments were performed at this TGFβ1 concentration.

To test the hypothesis that the addition of KGluc would inhibit fibroblast differentiation, fibroblasts were cultured with TGFβ1 and were further supplemented with increasing concentrations of KGluc. αSMA positive myofibroblasts were observed in all treatment groups (Figure 3 A–E), although few were observed in negative control fibroblasts (Figure 3A), and fibroblasts in differentiation medium with constant stimulation of 60 or 80 mM KGluc (Figure 3 C–D). There were a large number of αSMA positive myofibroblasts in positive controls without KGluc supplementation (Figure 3E), as well as with constant stimulation of 40 mM KGluc (Figure 3B). There was a reduction in the number of nuclei present in treatment groups constantly stimulated with 60 and 80 mM KGluc, as indicated by the proliferation data (Figure 1E), and the metabolic activity of fibroblasts from experiments cultured under similar conditions to the present experiment (Figure 1H). There was a significant reduction in the amount of αSMA expression in all culture conditions supplemented with KGluc with respect to positive controls (Figure 3F). While no significance was detected between concentrations of KGluc, there was a step-wise, downregulation of αSMA with increasing concentrations of KGluc. There was a significant difference in the αSMA expression from constant stimulation of 60 mM KGluc with late stimulation of 60 mM. To confirm that KGluc supplementation affected fibroblast differentiation and that this was not a hyperosmolar effect, we also cultured fibroblasts in sodium gluconate (NaGluc) and NDMG, a non-charged osmolar control (Supplementary Figure S2). There was a significant decrease in the αSMA expression between fibroblasts supplemented with KGluc with respect to controls as well as fibroblasts supplemented with NDMG or NaGluc. These data suggest that exogenous potassium, not hyperosmolarity itself or gluconate, are primarily affecting myofibroblast differentiation.

Together with the proliferation, metabolic activity, and migration data, we demonstrated that 60 mM KGluc was the minimal concentration required to observe inhibitory effects on some

fibroblast functions. Further, this concentration showed that sustained, constant stimulation significantly enhanced the inhibitory effects of KGluc on these cell functions with respect to late stimulation of KGluc. For these reasons, all future experiments in designing delivery mechanisms and *in vivo* delivery of KGluc for the aim of reducing scar formation incorporated 60 mM KGluc.

3.4. Collagen hydrogels are an effective delivery vehicle for treatment with potassium gluconate

To develop a clinically relevant delivery mechanism for KGluc, we assessed the feasibility of supplementing KGluc into collagen hydrogels. The concentration of KGluc added into the collagen gels was adjusted to deliver a final concentration of 60 mM, and from here two formations were used: KG-High and KG-Low (final gel concentrations of 1,000 and 500 mM of KGluc, respectively). The KG-Low condition was included as there were initial concerns that the high salinity within the gel solution could interfere with collagen gelation. One hundred microliters of this gel was added into transwells on top of fibroblasts previously in culture for three days (Figure 4A). While the KG-High condition gelled rapidly, there were no difficulties forming gels with any of the conditions. KGluc supplementation significantly inhibited myofibroblast conversion as measured via αSMA expression (Figure 4B). KG-Low inhibited myofibroblast conversion at a comparable level to 60 mM of soluble KGluc. KG-High supported qualitatively less αSMA expression than the soluble KGluc and KG-Low conditions and significantly less αSMA expression than negative controls.

To determine the effects of KGluc supplementation on fibroblast resting membrane potential (RMP), fibroblasts were patch clamped after exposure to KGluc or NMDG (control). KGluc treatment depolarized fibroblasts to an RMP of −9.5 ± 0.8, a significant increase from control fibroblasts that had an RMP of −14.3 ± 0.6 (Figure 5). These data indicate that the cell membrane was permeable to potassium (likely a result of the open state of native potassium carrying channels), and that KGluc supplementation was sufficient to alter the resting RMP by driving ionic movement across the membrane.

3.5. Effect of potassium gluconate in an *in vivo* model of wound healing

To determine the efficacy of KGluc to remodel injured skin, we generated a full thickness skin defect in mice and treated these wounds with collagen gels with or without KGluc. Two 8 mm diameter full thickness biopsies were removed from the dorsal skin of adult mice. On the left side wounds, 50 μL of collagen gels with KG-Low, KG-High, or DI water as a vehicle control were pipetted onto the wound and allowed to solidify (Figure 6A). The right side wounds remained untreated to serve as additional internal controls. Both wounds were sealed using Tegaderm, and wound progression was followed over the course of 14 days by quantifying the wound size (Figure 6B, Supplementary Figure S3). Before day 8, KGluc supplementation appeared to qualitatively delay wound closure, while after this time point the wounds rapidly closed faster than controls (Figure 6C). At day 6, KG-High-treated wounds were significantly larger than vehicle-treated controls.

To investigate the role of KGluc on wound regeneration and scar formation, we analyzed skin morphology 14 days after injury. All wounds treated with KGluc-loaded hydrogels were closed at this time, while some wounds treated with vehicle controls had not fully closed. Regenerated skin was harvested, bisected, and tissue sections were prepared using a cryotome. Tissue sections were immunostained for cytokeratin 10 (K10) to assess skin wound healing and to visualize the epidermal thickness and maturity. K10 is a protein present in keratinizing epithelium and is present in mature dermis.[20] Representative images revealed that dermal structures such as hair follicles or other glands did not penetrate into the dermal layer, while these features are readily observable in healthy skin (Figure 7A, double arrow). This allowed for the identification of the regenerating region of the tissue. Regardless of the lack of hair follicles, all wound sites showed the beginning of the formation of a dermal-epidermal junction (Figure 7 A–C, dotted lines). Control and KG-Low wound sites showed thick epidermal structures adjacent to mature skin (Figure 7A–B), while KG-High treated wounds showed a thin epidermis with a well formed, interdigitated dermal-epidermal interface (Figure 7C). There were some control samples that revealed nuclei above the epidermal structures (Figure 7A, arrowheads), suggesting the continued presence of a fibrin clot. It was noted that the presence of the keratinized layer of the epidermis was less fully formed at these locations. Quantification of the epidermal thickness demonstrated that KGluc lowered epidermal thickness, and that KG-High treatment significantly reduced epidermal thickness with respect to control injuries, approximating the thickness of mature, healthy skin (Figure 7D). All conditions had significantly larger epidermal thicknesses with respect to healthy mouse skin (21.9 ± 2.0 μm).

3.6. Potassium gluconate treatment reduces presence of dermal myofibroblasts *in vivo*

To determine the amount of myofibroblasts within the regenerating dermal tissue, tissue sections were immunostained for α smooth muscle actin (αSMA) 14 days post injury. As expected, αSMA staining was contained within the dermis, and revealed both myofibroblast populations as well as smooth muscle cell lined blood vessels (small-diameter arteries, arterioles, etc.). Representative images identified concentrations of myofibroblasts in the bulk of the dermal layer, as well as blood vessels throughout the dermis (Figure 8 A–C). There was also αSMA positive staining around some healthy skin structures, which were not included in the analysis of regenerating tissue. Control wounds expressed a continuous amount of positive αSMA stain throughout the injury site, indicating the presence of a large number of myofibroblasts (Figure 8A), while much less staining was present in KGluc treated wounds (Figure 8 B–C). KGluc treated wounds also presented a clearer dermal-epidermal junction, as identified by the appearance of a basal layer of keratinocyte stem cells/transient amplifying cells at the epidermal junction (dotted line). To measure the amount of myofibroblasts in the wound sites, we calculated the number of αSMA positive pixels within the wound sites, excluding healthy skin and skin structures, and normalized this to the number of nuclei within the area as measured by DAPI staining. KGluc treatment significantly reduced the amount of αSMA staining, indicating a significant reduction in the number of myofibroblasts within the dermis of these regenerating skin structures (Figure 8D). While there was less αSMA staining observed within the wound site, there appeared to be an increase in the number of αSMA positive stained blood vessels, as identified by their circular morphology (arrowheads) and the visualization of red blood cells. Quantification of

the number of blood vessels revealed that treatment with KGluc increased the blood vessel density, with there being a significantly higher density of blood vessels in KG-High treated wounds than control wounds (Figure 8E).

4. DISCUSSION

The goal of this study was to investigate the ability of hyperosmolar KGluc to inhibit myofibroblast conversion and ultimately reduce scar tissue formation. The lack of efficacy and problems associated with delivery of pharmacologic compounds maintains a compelling need to develop tissue engineered strategies aimed at the reduction of scar formation. Our approach to this clinical need has been to investigate ion-channel mediated signaling as a method to control cell phenotype. Ion flux has been shown to affect a variety of cell functions including development, homeostasis, regeneration, and tissue repair in mammalian systems.[15, 21] Alterations in potassium flux have been shown to modulate hMSC function, [10–11] and also are associated with changes in macrophage protein secretion.[22] We report a novel role of potassium flux on fibroblast proliferation which is in line with previous work characterizing hMSC proliferation in hyperosmolar potassium.[23] Importantly, hyperosmolar KGluc significantly reduced αSMA expression, and also resulted in a more mature epidermal layer as measured by a reduction in epidermal thickness as well as a more fully defined dermal-epidermal interface.

To analyze how hyperosmolar KGluc was affecting fibroblast phenotype, we patch clamped fibroblasts exposed to KGluc and measured the RMP. Our data demonstrate that, as expected, a potassium-dependent depolarization emerged upon introduction of hyperosmolar KGluc. The presence of increased extracellular potassium resulted in a reduction in the number of myofibroblasts in 2D cultures of ventricular fibroblasts.[24] Interestingly, this report indicates that low concentrations of extracellular potassium may increase the number of myofibroblasts, while elevated concentrations result in inhibition of myofibroblast differentiation. While our results did not investigate the effects of low concentrations of extracellular potassium beyond what is typically present in cell culture medium, a step-wise decrease in αSMA expression (i.e. a decrease in the number of myofibroblasts) was observed with increasing concentrations of KGluc, which is supported by previous work. Roach *et al.* determined that potassium flux signaling interfered with TGFβ1-mediated Smad2/3 phosphorylation, i.e. an increase in extracellular potassium inhibited receptor phosphorylation and therefore blocked Smad2/3 signaling.[25] We hypothesize is the mechanism by which hyperosmolar KGluc is suppressing myofibroblast differentiation. We assessed the contribution of hyperosmolarity to myofibroblast differentiation with other salts and verified that hyperosmolar controls (NDMG: non-charged control) and sodium ions (NaGluc) did not play as much of a role in myofibroblast differentiation. Taken together, our data suggest that (hyper)osmolarity plays a negligent role in myofibroblast differentiation, and that KGluc is likely inhibiting differentiation directly through TGFβ1 signaling.

An unexpected finding in this study was that KGluc treatment enhanced angiogenesis during wound healing of full thickness skin defects. To our knowledge, this is the first instance of application of KGluc to a skin wound. The introduction of additional ions may be affecting the endogenous electric field within the regenerating skin tissue, which has been shown to

affect endothelial cell alignment,[26] and has also been shown to signal endothelial cells through enhanced VEGF secretion.[26–28] If the addition of KGluc to the wound site alters endogenous electric fields within the regenerating skin tissue, this mechanism could support our observations of an increased presence of blood vessels. An alternate hypothesis is that KGluc could be stimulating other cells, such as macrophages, to stimulate pro-angiogenic factors by shifting macrophage polarization to the pro-wound healing M2-like phenotype.[22] Macrophage depolarization as a function of potassium flux modulation significantly reduced expression of the inflammatory protein tumor necrosis factor α (TNFα), and upregulated the expression of CD206, which is known to be associated with M2 polarization of macrophages.[29] The increase in blood vessel density could have further significance for the re-innervation of these tissues, as previous work has shown that endothelial cells secrete neurotrophic factors and are capable of directing targeted axonal growth in collagen-based systems.[17, 30] In a separate study where skin wounds were treated with ivermectin, ivermectin significantly altered fibroblast gene expression, resulting in increased dermal innervation and angiogenesis,[19] suggesting that KGluc-treated fibroblasts may also support an increased influx of blood vessels into the wound site. Further work is necessary to properly dissect the contributions of KGluc on enhancing angiogenesis; either through direct action on endothelial cells or through paracrine signaling with other cell types, such as through studying a model of ischemic tissue.[31]

It is interesting to note that while KGluc significantly enhanced blood vessel infiltration and significantly reduced the resident myofibroblast population within wound sites, there was less of an effect on the rate of wound closure. While the observed delay in wound closure might increase the potential risk of wound infection, binding the wound with Tegaderm as was done in this study may ameliorate this risk. These data may be attributable to the scratch assay results, which demonstrated that fibroblasts migrate slower in the presence of KGluc. This is important to note as keratinocytes will only migrate and re-epithelialize wounded skin after fibroblasts have remodeled the underlying dermis.[32] Therefore, the initial lag in wound closure may be a result of decreased fibroblast migration, although the reason for the rapid wound closure observed after day 7 is unclear. A possible explanation could be that these data result from the ability of BALB/c mice to heal and contract wound sizes relatively quickly.[33] Similar experiments could be performed on animal strains,[34] or diseased conditions such as diabetes, that are less associated with regenerative competency to more definitively identify the role of fibroblast migration on skin wound healing. Conversely, as stated above there may be paracrine-signaling effects present in KGluc treated wounds enhancing keratinocyte migration. Further work will need to be done to assess the contributions of potassium flux directly on these cell types and on the paracrine signaling events within the wound site.

5. CONCLUSIONS

In this study, we identified a role for KGluc treatment on the inhibition of myofibroblast differentiation and potentially for the preventative treatment of scar formation. KGluc significantly decreased fibroblast proliferation, migration, and differentiation with increasing concentrations, and can be delivered via collagen hydrogels *in vitro* and *in vivo*. Hyperosmolar conditions themselves did not affect fibroblast differentiation, suggesting a

role of potassium flux in this inhibition. KGluc treatment qualitatively delayed initial wound closure of a full-thickness skin injury; however, these wounds ultimately closed at the same time as vehicle controls. Further, KGluc treatment reduced the number of myofibroblasts present in the dermis, increased the density of blood vessels, and developed a more mature dermal-epidermal junction. Taken together, these data strongly support the continued investigation of KGluc as a preventative agent for scar formation.

Supplementary Material

Refer to Web version on PubMed Central for supplementary material.

ACKNOWLEDGEMENTS

The authors thank Joshua D. Erndt-Marino and Nicolas Rouleau for helpful discussions.

FUNDING

This research was funded in part by the NIH (P41-EB002520, R01-AR055993, F32-DE026058), the WM Keck Foundation, and the Allen Discovery Center program through The Paul G. Allen Frontiers Group (12171).

REFERENCES

1. Corona BT; Wu X; Ward CL; McDaniel JS; Rathbone CR; Walters TJ, The promotion of a functional fibrosis in skeletal muscle with volumetric muscle loss injury following the transplantation of muscle-ECM. Biomaterials 2013, 34 (13), 3324–35. [PubMed: 23384793]
2. Gawronska-Kozak B; Bogacki M; Rim JS; Monroe WT; Manuel JA, Scarless skin repair in immunodeficient mice. Wound Repair Regen 2006, 14 (3), 265–76. [PubMed: 16808805]
3. 2017 plastic surgery statistics report. American Society of Plastic Surgeons 2018.
4. Rahimnejad M; Derakhshanfar S; Zhong W, Biomaterials and tissue engineering for scar management in wound care. Burns Trauma 2017, 5, 4. [PubMed: 28127573]
5. Hinz B, Formation and function of the myofibroblast during tissue repair. J Invest Dermatol 2007, 127 (3), 526–37. [PubMed: 17299435]
6. Coentro JQ; Pugliese E; Hanley G; Raghunath M; Zeugolis DI, Current and upcoming therapies to modulate skin scarring and fibrosis. Adv Drug Deliv Rev 2018.
7. Jia S; Xie P; Hong SJ; Galiano R; Singer A; Clark RA; Mustoe TA, Intravenous curcumin efficacy on healing and scar formation in rabbit ear wounds under nonischemic, ischemic, and ischemia-reperfusion conditions. Wound Repair Regen 2014, 22 (6), 730–9. [PubMed: 25230783]
8. Garg K; Corona BT; Walters TJ, Losartan administration reduces fibrosis but hinders functional recovery after volumetric muscle loss injury. J Appl Physiol (1985) 2014, 117 (10), 1120–31. [PubMed: 25257876]
9. Li H; Duann P; Lin PH; Zhao L; Fan Z; Tan T; Zhou X; Sun M; Fu M; Orange M; Sermersheim M; Ma H; He D; Steinberg SM; Higgins R; Zhu H; John E; Zeng C; Guan J; Ma J, Modulation of wound healing and scar formation by MG53 protein-mediated cell membrane repair. The Journal of biological chemistry 2015, 290 (40), 24592–603. [PubMed: 26306047]
10. Sundelacruz S; Levin M; Kaplan DL, Depolarization alters phenotype, maintains plasticity of predifferentiated mesenchymal stem cells. Tissue Eng Part A 2013, 19 (17–18), 1889–908. [PubMed: 23738690]
11. Sundelacruz S; Levin M; Kaplan DL, Membrane potential controls adipogenic and osteogenic differentiation of mesenchymal stem cells. PLoS One 2008, 3 (11), e3737. [PubMed: 19011685]
12. Erndt-Marino JD; Jimenez-Vergara AC; Diaz-Rodriguez P; Kulwatno J; Diaz-Quiroz JF; Thibeault S; Hahn MS, In vitro evaluation of a basic fibroblast growth factor-containing hydrogel toward vocal fold lamina propria scar treatment. J Biomed Mater Res B Appl Biomater 2017.

13. Erndt-Marino J; Diaz-Rodriguez P; Hahn MS, Initial In Vitro Development of a Potassium-Based Intra-Articular Injection for Osteoarthritis. Tissue Eng Part A 2018, 24 (17–18), 1390–1392. [PubMed: 29562839]
14. Hart MR; Anderson DJ; Porter CC; Neff T; Levin M; Horwitz MS, Activating PAX gene family paralogs to complement PAX5 leukemia driver mutations. PLoS Genet 2018, 14 (9), e1007642. [PubMed: 30216339]
15. Sundelacruz S; Levin M; Kaplan DL, Role of membrane potential in the regulation of cell proliferation and differentiation. Stem Cell Rev 2009, 5 (3), 231–46.
16. Mene P; Pirozzi N, Potassium channels: the 'master switch' of renal fibrosis? Nephrol Dial Transplant 2010, 25 (2), 353–5. [PubMed: 19945954]
17. Grasman JM; Ferreira JA; Kaplan DL, Tissue Models for Neurogenesis and Repair in 3D. Adv Funct Mater 2018, 28 (48), 1803822.
18. Neher E, Correction for liquid junction potentials in patch clamp experiments. Methods Enzymol 1992, 207, 123–31. [PubMed: 1528115]
19. Cairns DM; Giordano JE; Conte S; Levin M; Kaplan DL, Ivermectin Promotes Peripheral Nerve Regeneration during Wound Healing. ACS Omega 2018, 3 (10), 12392–12402. [PubMed: 30411007]
20. Qu Y; Cao C; Wu Q; Huang A; Song Y; Li H; Zuo Y; Chu C; Li J; Man Y, The dual delivery of KGF and bFGF by collagen membrane to promote skin wound healing. J Tissue Eng Regen Med 2018, 12 (6), 1508–1518. [PubMed: 29706001]
21. McLaughlin KA; Levin M, Bioelectric signaling in regeneration: Mechanisms of ionic controls of growth and form. Dev Biol 2018, 433 (2), 177–189. [PubMed: 29291972]
22. Li C; Levin M; Kaplan DL, Bioelectric modulation of macrophage polarization. Scientific reports 2016, 6, 21044. [PubMed: 26869018]
23. Sundelacruz S; Li C; Choi YJ; Levin M; Kaplan DL, Bioelectric modulation of wound healing in a 3D in vitro model of tissue-engineered bone. Biomaterials 2013, 34 (28), 6695–705. [PubMed: 23764116]
24. Chilton L; Ohya S; Freed D; George E; Drobic V; Shibukawa Y; Maccannell KA; Imaizumi Y; Clark RB; Dixon IM; Giles WR, K+ currents regulate the resting membrane potential, proliferation, and contractile responses in ventricular fibroblasts and myofibroblasts. Am J Physiol Heart Circ Physiol 2005, 288 (6), H2931–9. [PubMed: 15653752]
25. Roach KM; Feghali-Bostwick C; Wulff H; Amrani Y; Bradding P, Human lung myofibroblast TGFbeta1-dependent Smad2/3 signalling is Ca(2+)-dependent and regulated by KCa3.1 K(+) channels. Fibrogenesis & tissue repair 2015, 8, 5. [PubMed: 25829947]
26. Bai H; Forrester JV; Zhao M, DC electric stimulation upregulates angiogenic factors in endothelial cells through activation of VEGF receptors. Cytokine 2011, 55 (1), 110–5. [PubMed: 21524919]
27. Zhao M; Bai H; Wang E; Forrester JV; McCaig CD, Electrical stimulation directly induces pre-angiogenic responses in vascular endothelial cells by signaling through VEGF receptors. J Cell Sci 2004, 117 (Pt 3), 397–405. [PubMed: 14679307]
28. Ud-Din S; Sebastian A; Giddings P; Colthurst J; Whiteside S; Morris J; Nuccitelli R; Pullar C; Baguneid M; Bayat A, Angiogenesis is induced and wound size is reduced by electrical stimulation in an acute wound healing model in human skin. PLoS One 2015, 10 (4), e0124502. [PubMed: 25928356]
29. Spiller KL; Koh TJ, Macrophage-based therapeutic strategies in regenerative medicine. Adv Drug Deliv Rev 2017, 122, 74–83. [PubMed: 28526591]
30. Grasman JM; Kaplan DL, Human endothelial cells secrete neurotropic factors to direct axonal growth of peripheral nerves. Scientific reports 2017, 7 (1), 4092. [PubMed: 28642578]
31. Shvartsman D; Storrie-White H; Lee K; Kearney C; Brudno Y; Ho N; Cezar C; McCann C; Anderson E; Koullias J; Tapia JC; Vandenburgh H; Lichtman JW; Mooney DJ, Sustained delivery of VEGF maintains innervation and promotes reperfusion in ischemic skeletal muscles via NGF/GDNF signaling. Mol Ther 2014, 22 (7), 1243–53. [PubMed: 24769910]
32. Vig K; Chaudhari A; Tripathi S; Dixit S; Sahu R; Pillai S; Dennis VA; Singh SR, Advances in Skin Regeneration Using Tissue Engineering. Int J Mol Sci 2017, 18 (4).

33. Davis TA; Amare M; Naik S; Kovalchuk AL; Tadaki D, Differential cutaneous wound healing in thermally injured MRL/MPJ mice. Wound Repair Regen 2007, 15 (4), 577–88. [PubMed: 17650103]

34. van den Borne SW; van de Schans VA; Strzelecka AE; Vervoort-Peters HT; Lijnen PM; Cleutjens JP; Smits JF; Daemen MJ; Janssen BJ; Blankesteijn WM, Mouse strain determines the outcome of wound healing after myocardial infarction. Cardiovasc Res 2009, 84 (2), 273–82. [PubMed: 19542177]

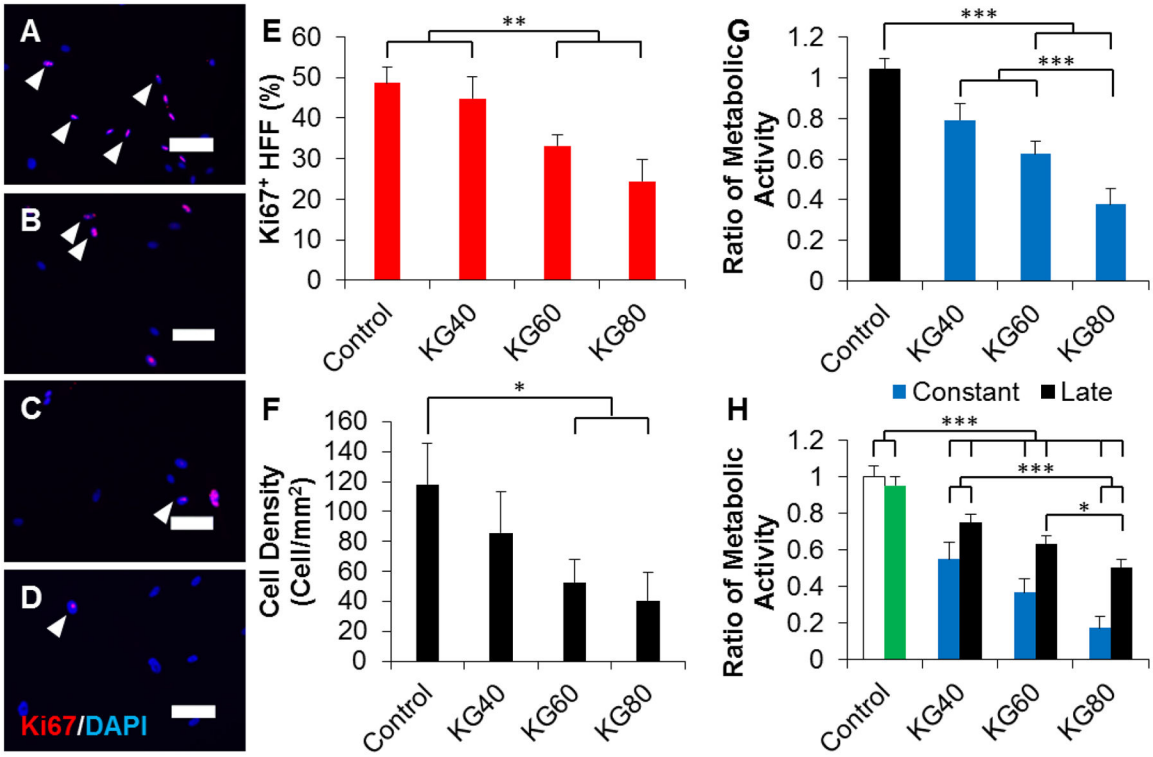

Figure 1.

Potassium gluconate inhibits fibroblast proliferation. (A-D) Representative images of fibroblasts cultured in (A) 0, (B) 40, (C) 60, and (D) 80 mM of exogenous potassium gluconate for 3 days. Arrowheads indicate representative Ki67 positive cells. Scale: 100 μm. (E) Quantification of the percentage of Ki67 positive fibroblasts. (F) Quantification of the density of fibroblasts cultured for 3 days in increasing concentrations of potassium gluconate. (G) Quantification of the metabolic activity of fibroblasts grown for 3 days in increasing concentrations of potassium gluconate. Data were normalized to the metabolic activity of control fibroblasts (black bar). (H) Quantification of the metabolic activity of fibroblasts cultured for 3 days with (constant) or without (late) potassium gluconate. After 3 days, fibroblasts were switched to differentiation medium with potassium gluconate. As controls, fibroblasts were not cultured in potassium gluconate either without differentiation medium (white bar, negative control), or with differentiation medium (green bar, positive control). Data were normalized to the metabolic activity of the negative control. * ($p<0.05$), ** ($p<0.01$), *** ($p<0.001$) and brackets indicate significance from other surfaces as determined by one-way ANOVA with Holm-Sidak post hoc analysis (n=5 independent experiments).

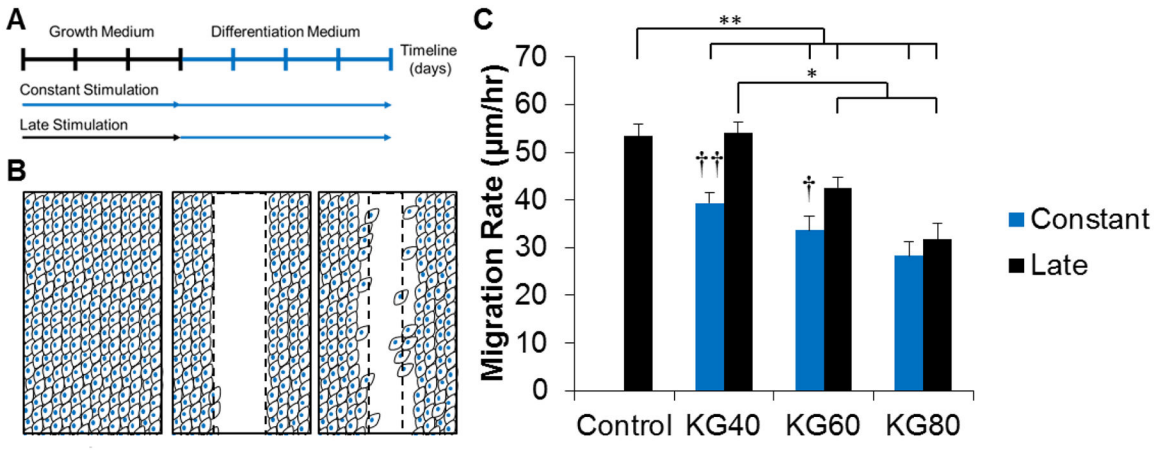

Figure 2.

Potassium gluconate reduces fibroblast migration. (A) Schematic of experimental design. Fibroblasts were either cultured for 3 days with (constant) or without (late) potassium gluconate. After 3 days, treatment was introduced with consistent concentrations of potassium gluconate. (B) Schematic of scratch assay. Confluent layers of fibroblasts were scratched with a P200 tip, creating a clear wound margin. The same locations were imaged every 4 hours to calculate the migration rate. (C) Quantification of migration rate. * ($p<0.05$), ** ($p<0.01$), and brackets indicate significance from other surfaces as determined by one-way ANOVA with Holm-Sidak post hoc analysis; and † ($p<0.05$) and †† ($p<0.01$) indicate significance between constant and late treatment groups within the same concentration of potassium gluconate as determined by Student's t-test (n=2 independent experiments).

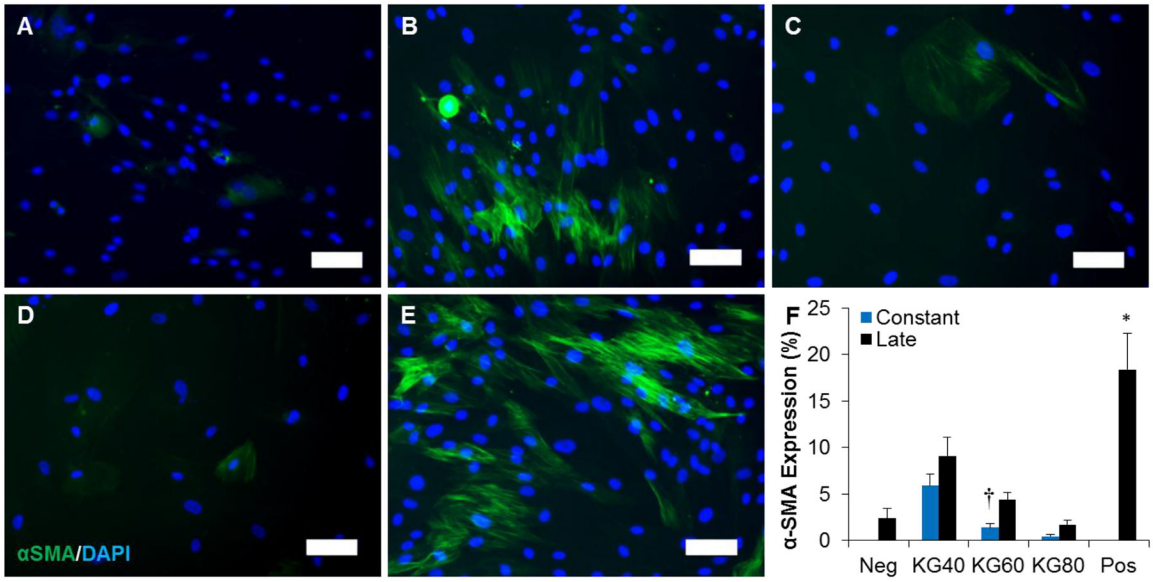

Figure 3.

Potassium gluconate inhibits fibroblast-myofibroblast differentiation. (A-E) Representative images of fibroblasts cultured with 1 ng/mL TGFβ1 supplemented with (B) 40, (C) 60, (D) 80, and (E) 0 mM (positive control) potassium gluconate. (A) Fibroblasts were also cultured with 0 ng/mL TGFβ1 and 0 mM potassium gluconate as a negative control. Scale: 100 μm. (F) Quantification of αSMA positive area. * ($p<0.05$) indicates significance with all other treatment groups as determined by one-way ANOVA with Holm-Sidak post hoc analysis and † ($p<0.05$) indicates significance between constant and late treatment groups within the same concentration of potassium gluconate as determined by Student's t-test (n=5 independent experiments).

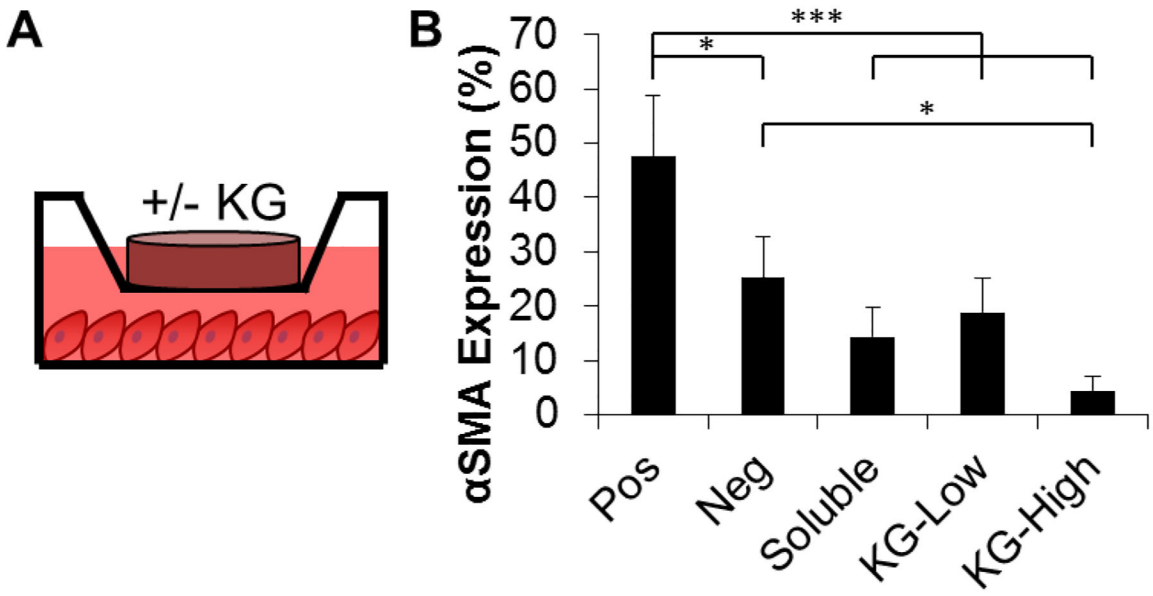

Figure 4.

Collagen gel is an effective delivery mechanism of potassium gluconate. (A) Schematic of experimental design. Collagen gels with or without potassium gluconate were placed in transwells on top of fibroblasts in differentiation medium. Positive controls have collagen gels with TGFβ1 and without potassium gluconate, while negative controls are not cultured with TGFβ1 or potassium gluconate. (B) Quantification of αSMA positive area. * ($p<0.05$), ** ($p<0.01$), *** ($p<0.001$) and brackets indicate significance between treatment groups as determined by one-way ANOVA with Holm-Sidak post hoc analysis (n=3 independent experiments).

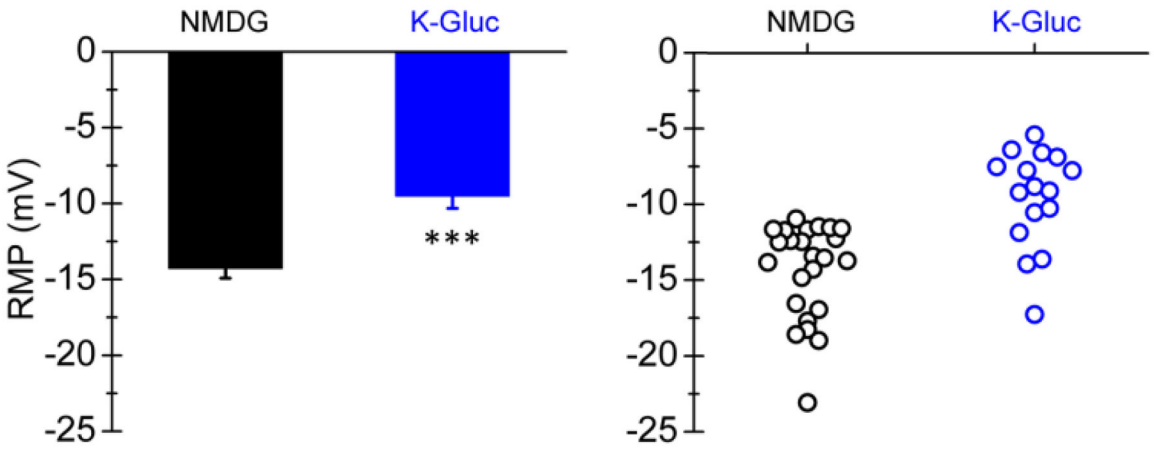

Figure 5.

Potassium gluconate depolarizes fibroblasts. Fibroblasts were exposed to NMDG (osmolar control) or KGluc, patch clamped, and the resting membrane potential was recorded. Each dot represents a distinct recording. *** ($p<0.01$) indicates significance between experimental conditions as determined by Students t-test ($n\geq4$ independent experiments).

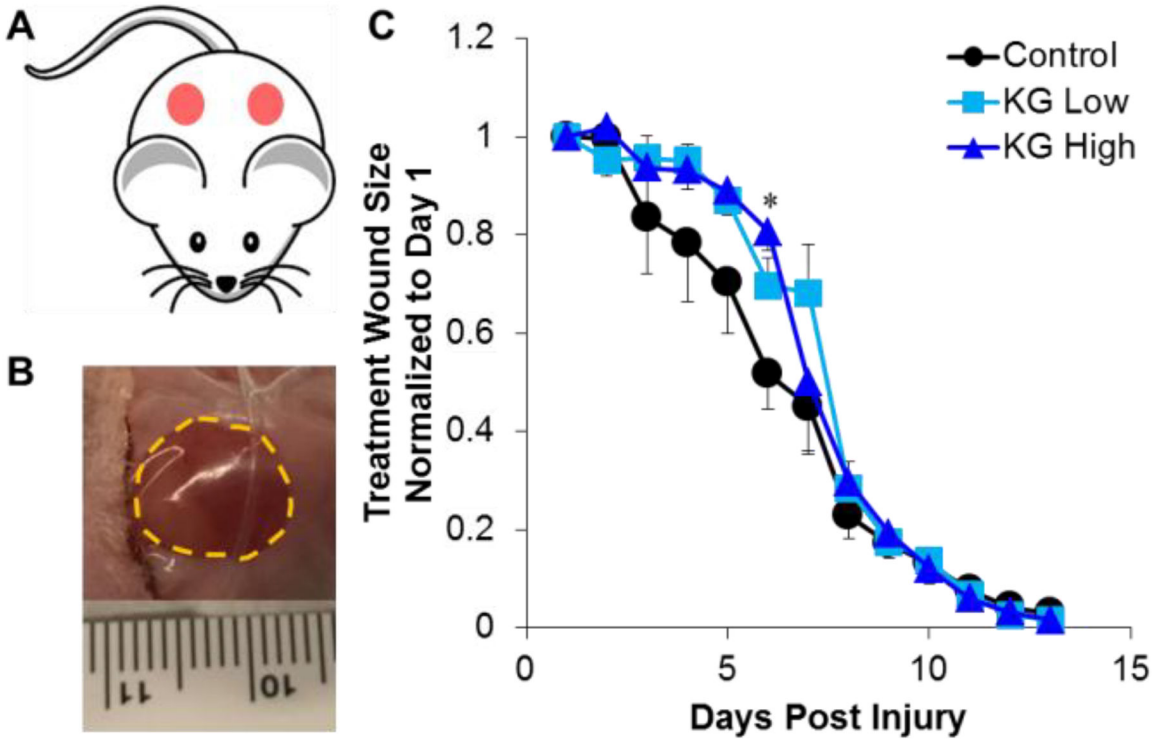

Figure 6.

Potassium gluconate delays early wound closure. (A) Schematic of experimental design. Two 8 mm full-thickness biopsies were taken from the dorsal skin of each mouse and 50 μL collagen gels with or without potassium gluconate were pipetted onto the left side wounds. The right side wounds remained untreated, and served as additional internal controls. Both wounds were sealed using Tegaderm, and (B) wound progression was followed over the course of 14 days. The area of the wound was measured and (C) quantified over time. * ($p<0.05$) indicates significance between experimental conditions as determined by one-way ANOVA with Holm-Sidak post hoc analysis (n=3).

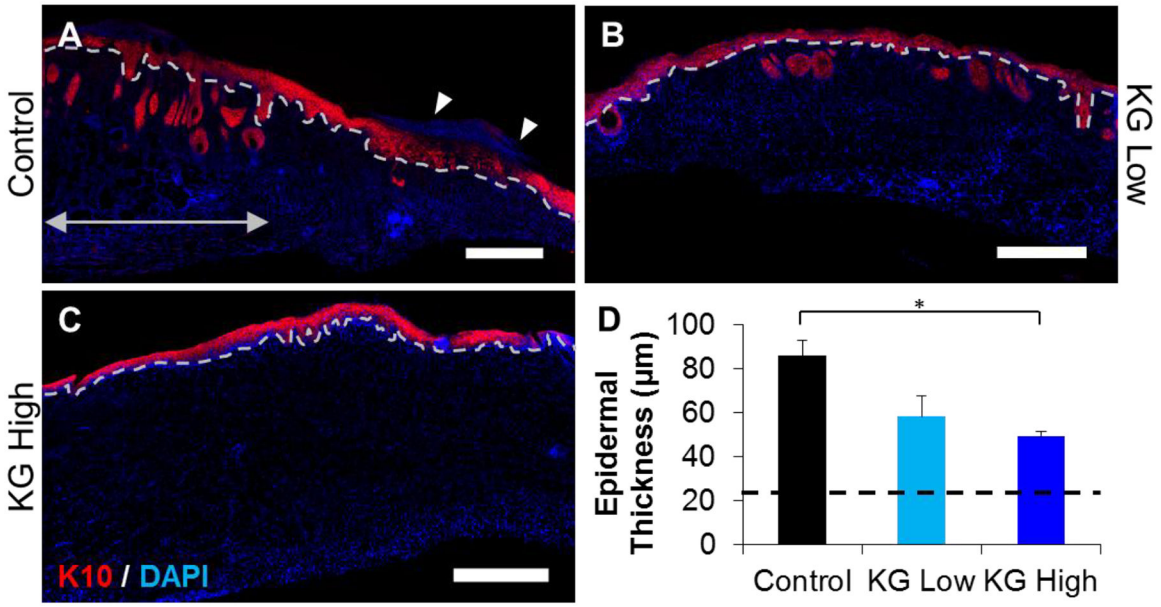

Figure 7.

Potassium gluconate reduces epidermal thickness and increases skin maturity. Cryosections of the wound sites were immunostained against cytokeratin 10 (K10). (A-C) Representative images of wound sites treated with (A) vehicle (control), (B) KG-Low, and (C) KG-High. Dotted lines indicate the dermal-epidermal junction. Double arrows indicate health tissue at the boundary of a wound site. Epidermal thickness was measured as the amount of K10 positive tissue above the dotted line. Scale: 500 μm. (D) Quantification of epidermal thickness as indicated by K10 expression. * ($p<0.05$), ** ($p<0.01$), and brackets indicates significance between indicated conditions as determined by one-way ANOVA with Holm-Sidak post hoc analysis (n=3).

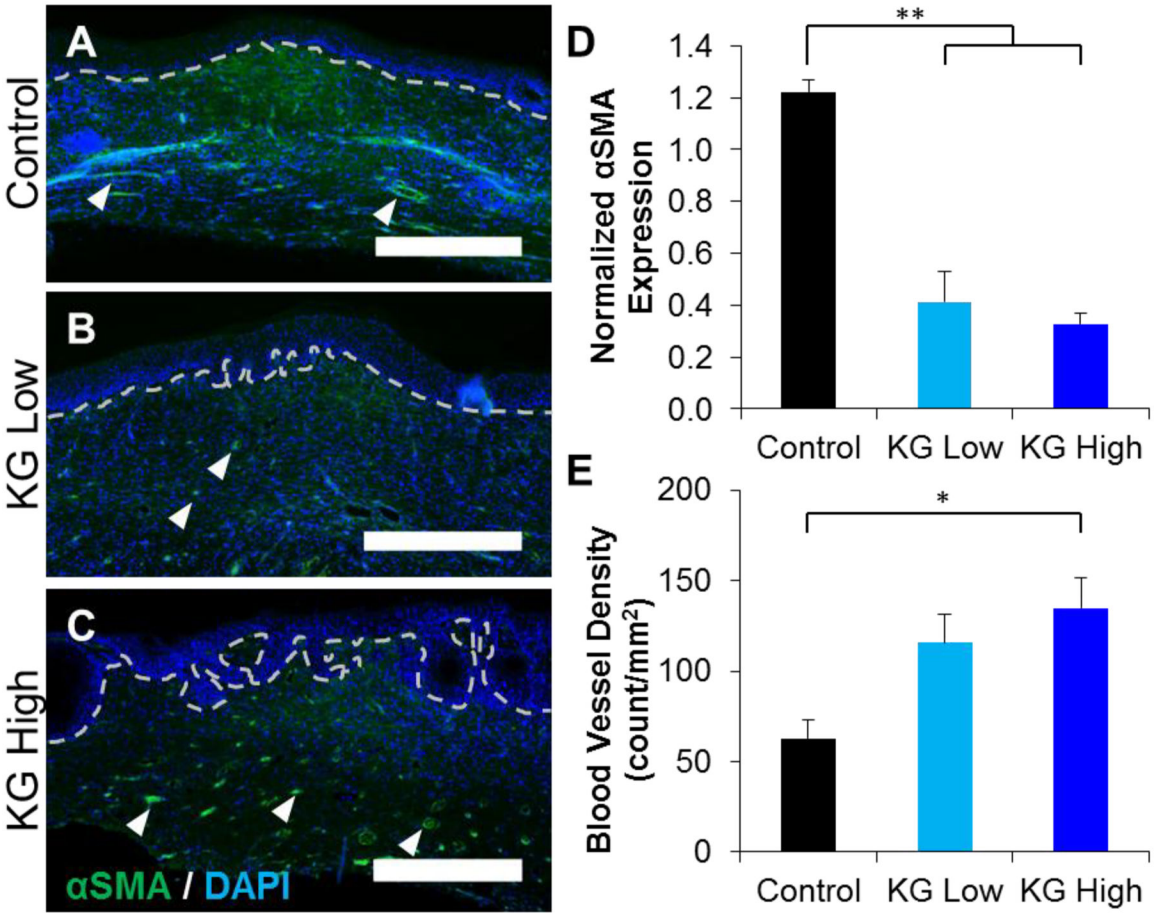

Figure 8.

Potassium gluconate reduces myofibroblast population and increases blood vessel density. Cryosections of the wound sites were immunostained against αSMA. (A-C) Representative images of wound sites treated with (A) vehicle (control), (B) KG-Low, and (C) KG-High. Dotted lines indicate the dermal-epidermal junction. Arrowheads indicate representative blood vessels. Scale: 500 μm. Quantification of (D) αSMA positive area in the wound site normalized to DAPI. (E) Quantification of the blood vessel density within wound sites. * ($p<0.05$), ** ($p<0.01$), and brackets indicates significance between indicated conditions as determined by one-way ANOVA with Holm-Sidak post hoc analysis (n=3).